NASA TN D-1258

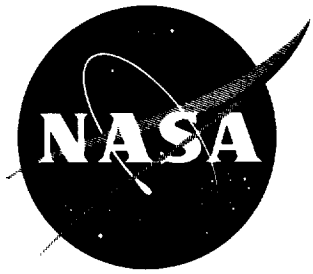

TECHNICAL NOTE

D-1258

INVESTIGATION OF THE RESPONSE OF MULTIWEB BEAMS TO STATIC AND DYNAMIC LOADING

By Wilbur B. Fichter and Eldon E. Kordes

Langley Research Center
Langley Station, Hampton, Va.

NATIONAL AERONAUTICS AND SPACE ADMINISTRATION
WASHINGTON May 1962

NATIONAL AERONAUTICS AND SPACE ADMINISTRATION

TECHNICAL NOTE D-1258

INVESTIGATION OF THE RESPONSE OF MULTIWEB BEAMS TO STATIC AND DYNAMIC LOADING

By Wilbur B. Fichter and Eldon E. Kordes

SUMMARY

Measured cover stresses are presented for four multiweb beams subjected to static uniform loading and four corresponding beams subjected to transient uniform loading. Elementary beam theory more accurately predicted the bending stresses due to static loading than those due to transient loading. Timoshenko beam theory offered no improvement over elementary theory for the one beam considered. Results for one specimen indicate that dynamic effects on the strength of multiweb beams can be appreciable.

INTRODUCTION

Multiweb beams are used extensively in the construction of high-speed aircraft and are applicable to the glider type of reentry vehicle. In such structures, beams are subjected not only to static loads but also to rapidly applied loads due to gusts, blasts, and so forth. Thus, while static stresses in built-up beams have been the subject of much research (see, for example, refs. 1 to 4), there is also a need for studying the response of such beams to rapidly applied loading. Further, it is of interest to indicate the usefulness of beam theory in predicting the stress response of such built-up structures and the magnitude of dynamic effects on their strength.

For these reasons, several multiweb beams have been subjected to static and dynamic loading. Unique testing techniques were employed for both types of loading. Uniform static lateral loading was achieved with a hydraulic device, and nearly uniform transient loading was achieved through the use of a pressurized chamber. Bending stresses were measured and compared with stresses calculated by means of beam theory. The theoretical calculations were based on the measured loading histories. The results are presented in this paper.

SPECIMENS AND INSTRUMENTATION

The multiweb beams were fabricated of 2024-T3 aluminum alloy and consisted of two cover sheets riveted to six formed-channel webs. A sketch of a typical specimen is shown in figure 1. All beams were of rectangular planform with a constant width of 10 inches and a constant length of 29 inches. Variables were depth, cover-sheet thickness, and web thickness. Other pertinent dimensions are given in table I for all multiweb specimens.

One specimen differed greatly from the others in the formation of one of its covers. Instead of a complete cover sheet, six 1-inch-wide strips were riveted to the channel webs along one surface of the beam. At each end of the beam a partial cover sheet was riveted to the strips; thus, the middle of that surface was left uncovered except for the six 1-inch-wide strips.

Instrumentation consisted of 1-inch and 6-inch resistance strain gages bonded to the cover sheets at the midspan of the beam (a typical arrangement is shown in fig. 1) and, in the transient loading tests, an NASA model 49TP miniature differential pressure gage. The strain gages were placed symmetrically with respect to the longitudinal axis of the beam; the 6-inch gages were as near as possible to the rivet lines and the 1-inch gages were midway between the rivet lines.

Generally, because of space limitations, strain gages could not conveniently be mounted on the inside surface of a cover. However, on the beam with the partial cover sheets, henceforth designated as specimen 1, three 1-inch gages were mounted on the inside surface of the full cover directly opposite three 1-inch gages on the outside surface in order to obtain values of average stress in the cover. These average stresses were found to be in good agreement with stresses measured with the 6-inch gages.

In addition to the multiweb beams, two solid beams with the same planforms as the multiweb beams were constructed. One beam (see fig. 2) was of SAE 4130 steel, 2 inches thick, and was instrumented with 18 NASA model 49TP miniature differential pressure gages modified to measure pressures on both surfaces of the beam. This beam was constructed for the purpose of obtaining data on some of the characteristics of the transient-loading device.

The other solid beam (see fig. 3) was of 2024-T3 aluminum alloy, 0.75 inch thick, and was instrumented with three miniature differential pressure gages and several types of resistance strain gages. This beam was constructed for the purpose of comparing its dynamic behavior with that of the multiweb beams.

TEST EQUIPMENT AND PROCEDURE

Dynamic Tests

Before a study of the response of multiweb beams to dynamic loading could be carried out, a method of rapidly applying loads to a beam had to be devised. It was also desired that the transient loading be essentially uniform. With these considerations in mind, the test fixture shown in figure 4 was devised. Also shown in figure 4 are two high-speed cameras used to photograph the beam motion during a test.

The test chamber was built from a standard T-shaped pipe having a 16-inch diameter with the base and hold-down flanges fitted to the leg of the T to accommodate a replaceable aluminum rupture diaphragm. Heavy end plates housing plate-glass windows to provide visual access for the high-speed cameras were fitted to the other two openings. Below the base and hold-down flanges and rupture diaphragm was a heavy baffle plate added to reduce blast noise. This baffle plate also served as a platform for an air-powered solenoid-operated puncturing device used to pierce the diaphragm and thereby initiate a test. Shown in figure 5 is a sketch of the test chamber showing side fairings added to decrease the air gaps between the chamber walls and the specimen, which was mounted horizontally and extended from one window to the other. Also shown are the quartz-tube lamps mounted on the chamber ceiling to provide sufficient light for the high-speed cameras. The specimen was simply supported by a shaft and bearings at each end. The bearings at one end of the beam were fitted into 1-inch-thick steel blocks machined for a tight fit with the bearings. At the other end the bearings rolled in a channel machined in 1-inch-thick steel blocks, which allowed longitudinal motion of that end of the beam and prevented vertical motion.

The test procedure consisted of first pressurizing the entire chamber to a desired value, then activating the recording equipment, lamps, cameras, and diaphragm-puncturing device in the desired sequence by a common timer. Puncturing of the aluminum diaphragm caused it to rupture violently and thus allowed that part of the chamber below the specimen to evacuate rapidly. Since the air gaps between the specimen and the chamber walls were small, the upper portion of the chamber evacuated less rapidly and a transient differential pressure across the specimen resulted. During a test, continuous records of differential pressure and beam bending strains were obtained.

All instrument leads from the specimen were connected to the recording equipment through an airtight plug located in one door of the chamber. Recording equipment, in addition to the high-speed cameras, consisted of 3-kc and 20-kc carrier amplifiers and an oscillograph recorder equipped with a high-speed-film drum capable of paper speeds up to 600 inches per second.

Several preliminary tests were performed by using the steel calibration beam in order to determine the pressure distribution over the surface of the beam as well as the relationship between initial chamber pressure and maximum differential pressure. Distribution of differential pressure over the surface of the beam during a typical test on the steel calibration beam is shown in figure 6. The distribution is seen to be nearly uniform as differential pressure increases and somewhat less than uniform as differential pressure decreases.

Figure 7 shows some typical histories of average differential pressure from tests on the steel calibration beam as well as the histories of pressure experienced at a representative location on the four multiweb specimens. The theoretical calculations were based on these measured pressure histories. For the pressure range covered in the tests, a value for peak differential pressure of about six-tenths to seven-tenths of initial chamber pressure could be expected.

With the completion of a nondestructive test on a multiweb beam, it was necessary only to install a new rupture diaphragm before performing another test on the same beam. Some tests, however, resulted in destruction of the specimen. Figure 8 is a closeup view of a beam blown out of the chamber when it was subjected to differential pressure somewhat greater than design maximum pressure. Protruding through the beam is the diaphragm-puncturing device minus the shaft and point, which were broken off by the beam. This test apparatus was operated at chamber pressures up to 100 psi with average loading rates up to 10,000 psi/sec.

Static Tests

In order to form a basis for comparison, it was necessary to devise a test fixture with which uniform static loading could be applied to the multiweb beams. That test fixture plus a low-capacity, high-pressure hydraulic pump for applying the load, an electrical pressure gage for load measurement, and a 24-channel recorder for obtaining continuous records of strain and pressure during a test comprised the static-test equipment. A view of the test fixture, containing a buckled specimen, is shown in figure 9. A steel shaft through each end of the beam, centered on the neutral axis, was held by bearings, which were free to rotate at both ends and to displace longitudinally at one end of the beam and thus effect simple-support conditions. Vertical deflections of the bearings were not allowed. Shown in addition to the test fixture are the hydraulic feeder line, a mechanical pressure gage for rough visual checks of the load, and the more accurate electrical pressure gage. Also shown are three cantilever gages and one of several dial gages used to measure beam deflections.

In order to apply a uniform load, hydraulic oil was pumped through the feeder line into an airtight cavity between the fixture base plate and a neoprene diaphragm which caused the diaphragm to bear uniformly against the beam. In this manner pressure was increased, with continuous recording of strain and pressure, until the specimen buckled. This test apparatus was operated at uniform pressures up to 110 psi.

Note that this testing procedure is unusual in that it produces true uniform lateral loading and, hence, provides a variable bending moment with a maximum at the center of the beam. Most previous static bending tests of multiweb beams have been under conditions of pure moment.

EXPERIMENTAL RESULTS AND COMPARISONS WITH BEAM THEORY

For the static tests, stresses were calculated by using elementary beam theory. (See ref. 5.) For the transient-loading tests, stresses were calculated by using a Williams type one-mode solution with elementary beam theory. (See, for example, ref. 6.) In addition, for specimen 3, stresses were calculated using a Williams type one-mode solution with Timoshenko beam theory, which includes the effects of transverse shear and rotary inertia. The parameters necessary for elementary theoretical calculations and their numerical values for the beams tested are given in table II. In the calculations, the mass per unit length of the beams was determined by multiplying the mass density of the material, which was the same $\left(2.59 \times 10^{-4}\ \text{lb-sec}^2/\text{in.}^4\right)$ for all aluminum beams tested, by the cross-sectional areas of the beams.

Static Tests

Four multiweb beams were subjected to static uniform loading. Bending stresses were recorded and are plotted in figure 10 against uniform pressure up to a value slightly below initial buckling pressure. In figure 10(a) separate curves are presented for the average of each pair of back-to-back 1-inch strain gages, and for the average of the pair of 6-inch strain gages on each cover sheet. Note in figure 10(a) that the average of all the data for the 1-inch strain gages is in good agreement with the average of the data for the two 6-inch strain gages on the same (compression) cover. From this observation it was assumed that, for practical purposes, the average of the 6-inch strain gages on each cover was representative of the average bending stress in that cover. Hence, on specimens other than specimen 1, 6-inch strain gages were used to obtain average stress readings, and 1-inch strain gages were mounted singly on both covers and were used only to more accurately

detect buckling. In the remainder of figure 10, only the curves for the averages of the 6-inch strain gages are presented. The experimental tensile and compressive stresses are compared with stresses calculated from elementary beam theory.

In figure 10, the horizontal dashed line on each figure denotes the initial buckling pressure. As a point of interest, the experimental average compressive stresses in the covers at buckling were compared with the values of buckling stress predicted in reference 3, with corrections for rivet offset obtained from results of the analysis in reference 4. This comparison is shown in table III. Three of the four specimens buckled at stresses lower than the predicted values (approximately 10 percent lower in three cases) whereas one specimen buckled at a stress value near and probably above the predicted value. The uncertainty as to the exact predicted value arises from the fact that the channel webs in that particular specimen were not of uniform thickness; whereas, the analysis of reference 4 is based on the assumption of uniform channel-web thickness. A possible reason for the disagreement with the results of references 3 and 4 is that the results of reference 3 are obtained under the condition of pure moment; hence, no transverse shear stress is present, nor does the moment vary over the length of the beam. In the present tests, of course, the moment does vary and the webs and cover sheets carry transverse shear.

L
1
3
5
7

As would be expected in bending tests of multiweb beams by uniform loading, some chordwise variation in the measured cover-sheet stresses was observed, as may be seen in figure 10(a). The variations in cover-sheet stresses can be attributed primarily to "secondary beam bending effects" such as shear lag and chordwise bending. Evidence of the chordwise bending effect is given in figure 11, where deflections at three equally spaced points across the midspan are plotted against uniform pressure for specimen 2. Deflection at the midchord is seen to be about 16 to 18 percent greater than at the edges.

Note in figure 10 that elementary beam theory predicted the average cover-sheet stresses with a tendency to be slightly conservative for the first three specimens. The results of these tests verify that elementary theory is useful for rough design calculations of bending stresses in multiweb beams subjected to static loading. However, in order to predict the detailed stress distribution, more refined theory must be employed.

Dynamic Tests

Four multiweb beams, each identical to a corresponding static-test specimen, were subjected to transient loading. Representative loading histories for these four specimens are shown in figure 7. The same

instrumentation as in the static tests was used except for the addition of a miniature differential pressure gage to each specimen.

Chordwise variations in cover-sheet bending stresses were generally no greater than in the static tests but were somewhat time dependent probably because of the nonuniform chordwise mass distribution. As in the static tests, specimen 3 (the deepest of the four beams) exhibited the least chordwise variation in cover-sheet stresses.

Stress histories from the tests on four multiweb beams are presented in figure 12 and compared with stresses calculated by using a Williams type one-mode solution with elementary beam theory. In addition, for specimen 3, a Williams type one-mode solution based on Timoshenko beam theory was employed.

L
1
3
5
7

The experimental results presented in figure 12 consist of curves for average tensile and average compressive stresses in the cover sheets. The calculated results consist of essentially single curves except for cases in which the calculated stresses were above the proportional limit of the material in compression. In these instances, the compressive stresses were corrected simply by reducing the elastic stress (at a given strain) to the actual value given by the stress-strain curve for the material. As a rule the tensile stresses needed no correction since the proportional limit of the material in tension is considerably higher. Similar corrections were made on the experimental compressive stresses whenever the material underwent strains beyond the proportional limit.

Agreement between experimental and calculated stresses is fairly good for three of the four specimens except near peak response. The overall agreement between experiment and theory is best for specimen 3 which, because of its greater depth-to-width ratio, was least susceptible to the effects of chordwise bending and shear lag. The results for specimen 3 also indicate that the multiweb beams tested were not greatly affected by transverse shear and rotary inertia since stresses calculated with Timoshenko beam theory, which takes these effects into account, were not appreciably different from those calculated by means of elementary beam theory; and specimen 3, the deepest of the four multiweb beams, should have been most susceptible to these particular effects.

Since Timoshenko beam theory does not account for the major differences between elementary beam theory and experiment, it is evident that secondary effects other than transverse shear and rotary inertia must be taken into account if more accurate predictions of multiweb beam response are to be made. It is felt that chordwise bending and shear lag were of about equal importance in the static and dynamic tests. A secondary effect present only in the dynamic tests could be called a "longitudinal inertia" effect. When a beam is undergoing rapid, fairly

large lateral displacements, as was the case with the more shallow beams, then transient longitudinal displacements and accelerations can result in axial neutral surface stresses even though both ends of the beam are not restrained axially. These transient middle-surface stresses can cause significant deviations from the elementary beam bending response.

In figure 12(d) the experimental curves for specimen 4 are not extended past a peak stress because slight buckling of the webs occurred. Note from figures 7 and 12(d) that buckling occurred in this specimen at a peak transient pressure of only 23 psi, whereas it sustained static pressure up to 28 psi before buckling, as is shown in figure 10(d). This result indicates that dynamic effects on the strength of multiweb beams can be appreciable.

Supplementary to the tests on multiweb beams, similar tests were performed on the solid aluminum beam, which is virtually free of shear lag and chordwise bending, to determine how much of the measured-stress variation across the width and how much of the disagreement with theory were due to secondary effects. The results of a typical test are presented in figure 13 where they are compared with the Williams type one-mode solution of reference 6. Agreement between calculated and measured stresses is generally better than that observed in the tests on multiweb beams, and less variation appears in the experimental data. This result seems to confirm that much of the variation in measured stresses and much of the disagreement with theory in the tests on multiweb beams are due to the secondary bending effects discussed previously.

For the sake of completeness it should be pointed out that another possible source of disagreement between theory and experiment is the assumption that the loading is always uniform. (See fig. 6.) In addition, a slight error results from the use of only the contribution of the first mode in the calculations; however, examination of the series for moment shows that this error is on the order of 4 percent or less.

CONCLUDING REMARKS

The results of an experimental investigation of the stress response of multiweb beams to static and dynamic loading are presented. Unique testing techniques were employed for both types of loading. Uniform static lateral loading was achieved with a hydraulic device in which the pressure was transmitted to the beam surface through a flexible diaphragm; thus, a moment which varied continuously along the length of the beam was applied. Nearly uniform transient pressure loading was achieved through the use of a pressurized chamber in which the chamber space on one side of the beam was suddenly evacuated.

Measured stresses in the beam cover sheets are compared with stresses calculated from elementary beam theory and, for one beam, Timoshenko beam theory. It is demonstrated that elementary beam theory may be useful for rough design calculations of bending stresses due to static uniform loading but for transient loading both elementary and Timoshenko beam theories yield unconservative results for the more flexible beams. For multiweb beams, Timoshenko theory offered little improvement over elementary theory. Results for one specimen indicate that dynamic effects on the strength of multiweb beams can be appreciable.

Langley Research Center,
National Aeronautics and Space Administration,
Langley Air Force Base, Va., February 20, 1962.

REFERENCES

1. Pride, Richard A., and Anderson, Melvin S.: Experimental Investigation of the Pure-Bending Strength of 75S-T6 Aluminum-Alloy Multiweb Beams With Formed-Channel Webs. NACA TN 3082, 1954.

2. Anderson, Roger A., Pride, Richard A., and Johnson, Aldie E., Jr.: Some Information on the Strength of Thick-Skin Wings With Multiweb and Multipost Stabilization. NACA RM L53F16, 1953.

3. Schuette, Evan H., and McCulloch, James C.: Charts for the Minimum-Weight Design of Multiweb Wings in Bending. NACA TN 1323, 1947.

4. Semonian, Joseph W., and Peterson, James P.: An Analysis of the Stability and Ultimate Compressive Strength of Short Sheet-Stringer Panels With Special Reference to the Influence of the Riveted Connection Between Sheet and Stringer. NACA Rep. 1255, 1956. (Supersedes NACA TN 3431.)

5. Timoshenko, S.: Strength of Materials. Part I - Elementary Theory and Problems. Second ed., D. Van Nostrand Co., Inc., 1940.

6. Leonard, Robert W.: On Solutions for the Transient Response of Beams. NASA TR R-21, 1959. (Supersedes NACA TN 4244.)

TABLE I.- CROSS-SECTIONAL DIMENSIONS OF MULTIWEB BEAMS

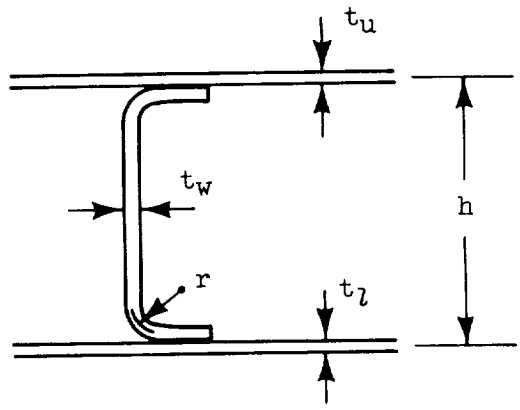

Specimen	Dimensions					
	h, in.	t_w, in.	t_u, in.	t_l, in.	t_s, in. (a)	r, in.
1	1.064	0.040	0.064	0.032	0.104	0.10
2	.936	.040	.064	.064		.10
3	1.939	.032	.064	.064		.14
4	.801	.030	.051	.051		.10

[a]Thickness of partial cover sheets on one side of beam.

TABLE II.- VALUES OF CONSTANTS USED IN NUMERICAL CALCULATIONS

[l = 26.5 in.; E = 10.6×10^6 psi]

Specimen	I_x, in.^{4}	A, in.^{2}	m, lb-sec^2/in.^{2}
1	0.365	1.75	4.53×10^{-4}
2	.344	1.71	4.43
3	1.408	1.77	4.59
4	.262	1.56	4.04
Solid beam	.352	7.50	19.4

where

I_x moment of inertia of beam cross section, in.^{4}

A cross-sectional area of beam, in.^{2}

m mass of beam per unit length, lb-sec^2/in.^{2}

l length of beam between supports, 26.5 in.

E modulus of elasticity, 10.6×10^6 psi

TABLE III.- BUCKLING STRESSES OF MULTIWEB BEAMS

Specimen	Buckling stress, ksi	
	Reference 3	Experimental
1	41.5	37.7
2	41.5	37.0
3	33.6	30.7
4	[a]28 to 36.3	37.0

[a]Exact value could not be determined due to nonuniform web thickness.

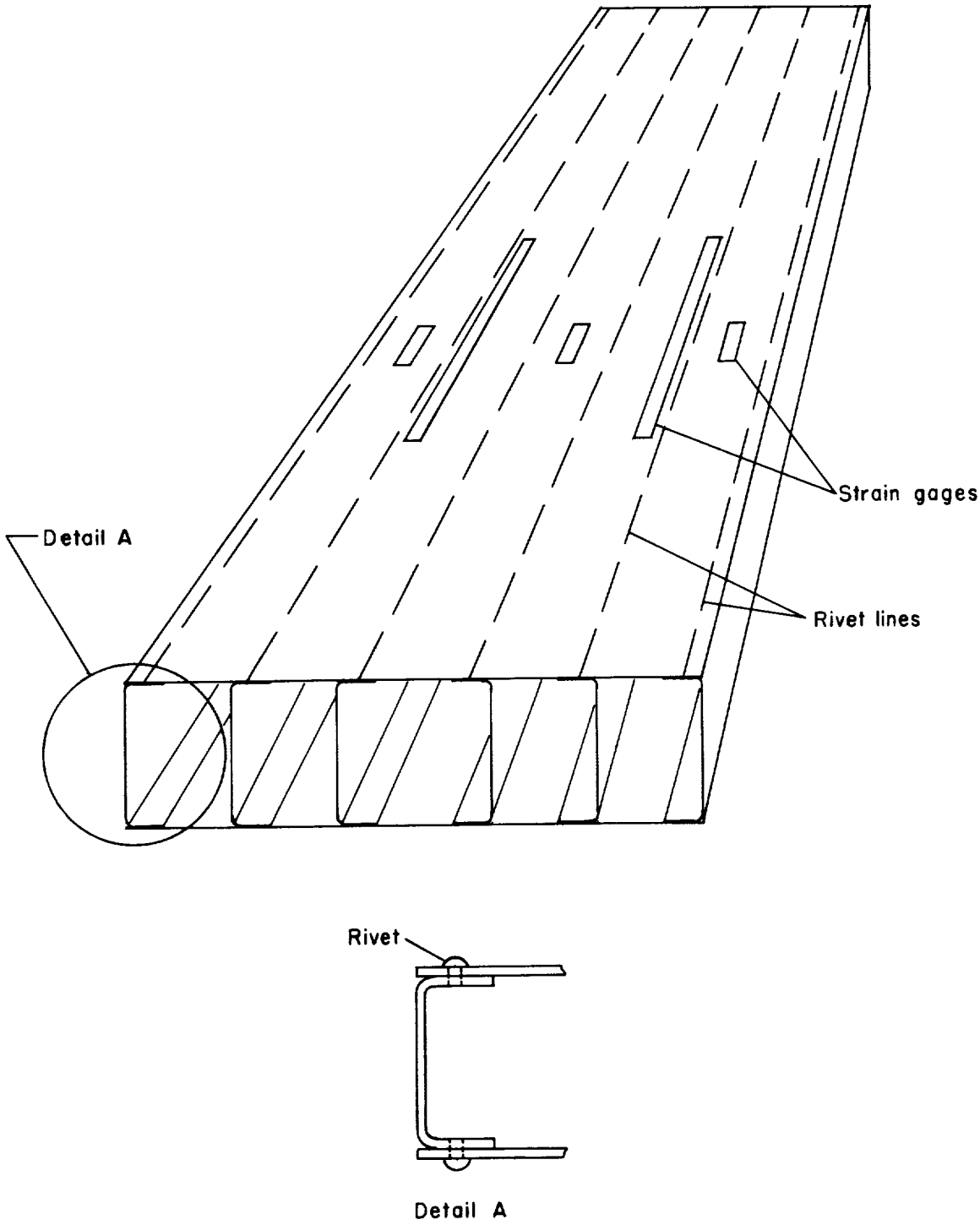

Figure 1.- Typical test specimen.

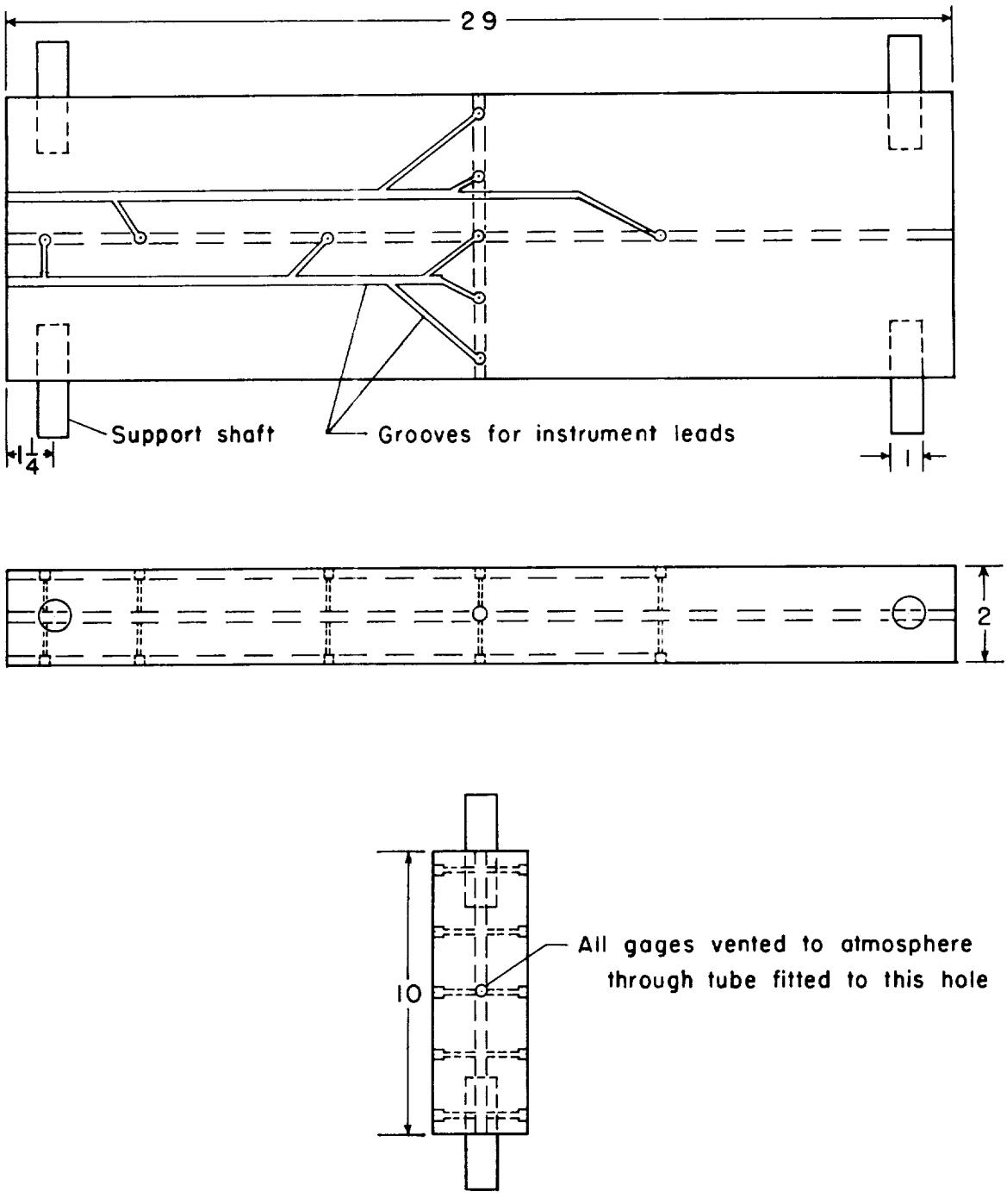

Figure 2.- Sketch of steel calibration beam showing pressure-gage locations. All dimensions in inches.

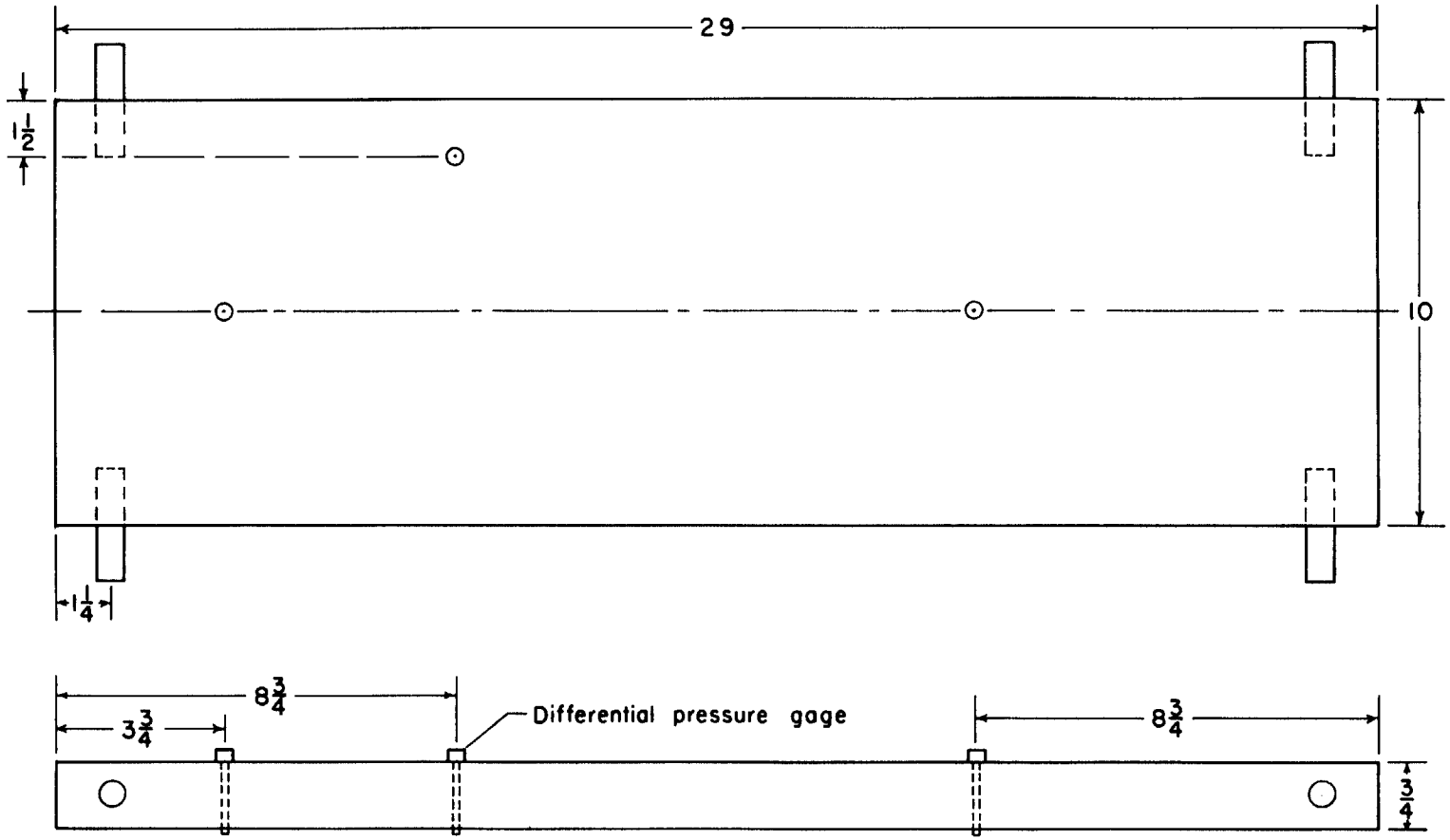

Figure 3.- Solid aluminum beam. All dimensions in inches.

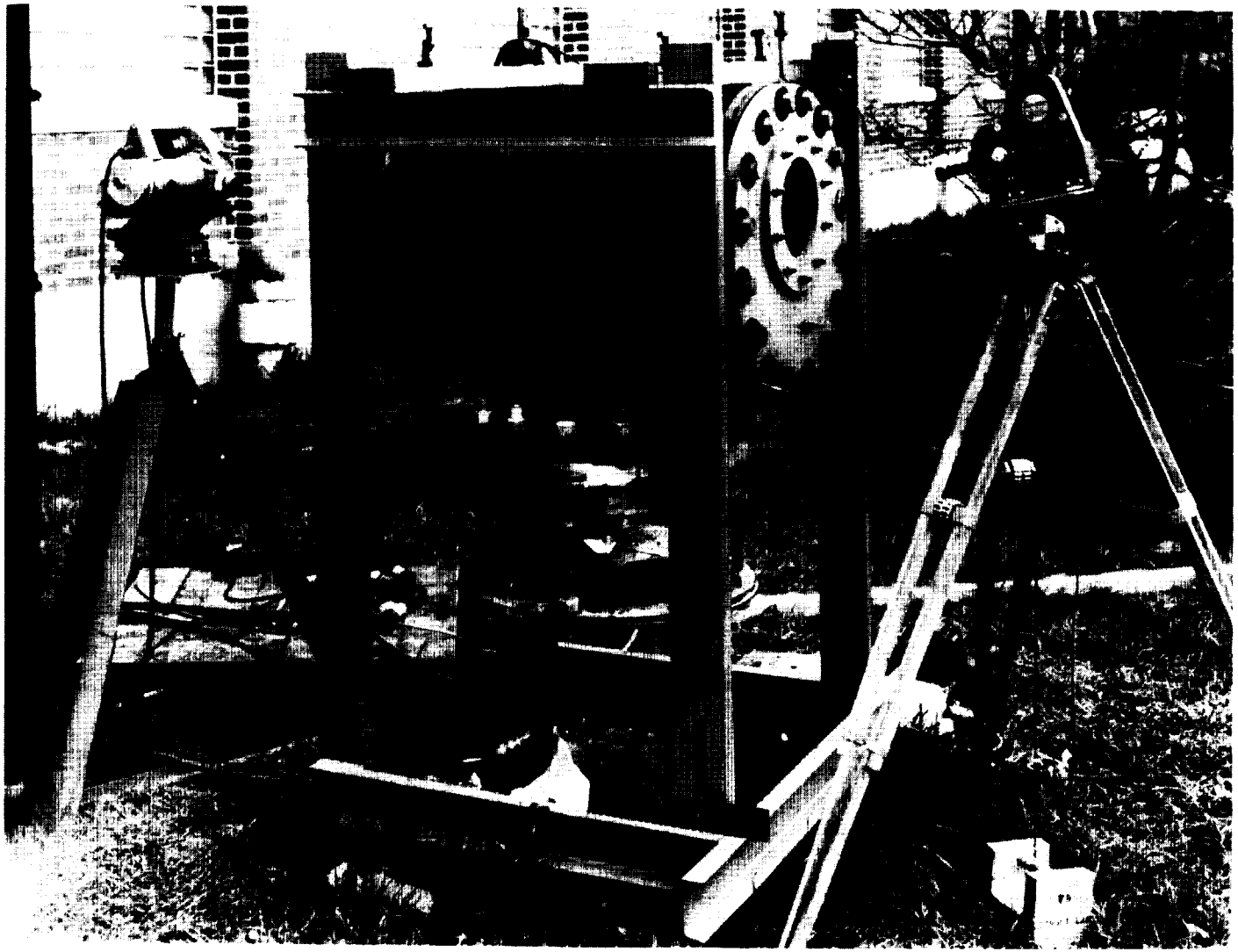

Figure 4.- Dynamic-test fixture and cameras. L-57-982

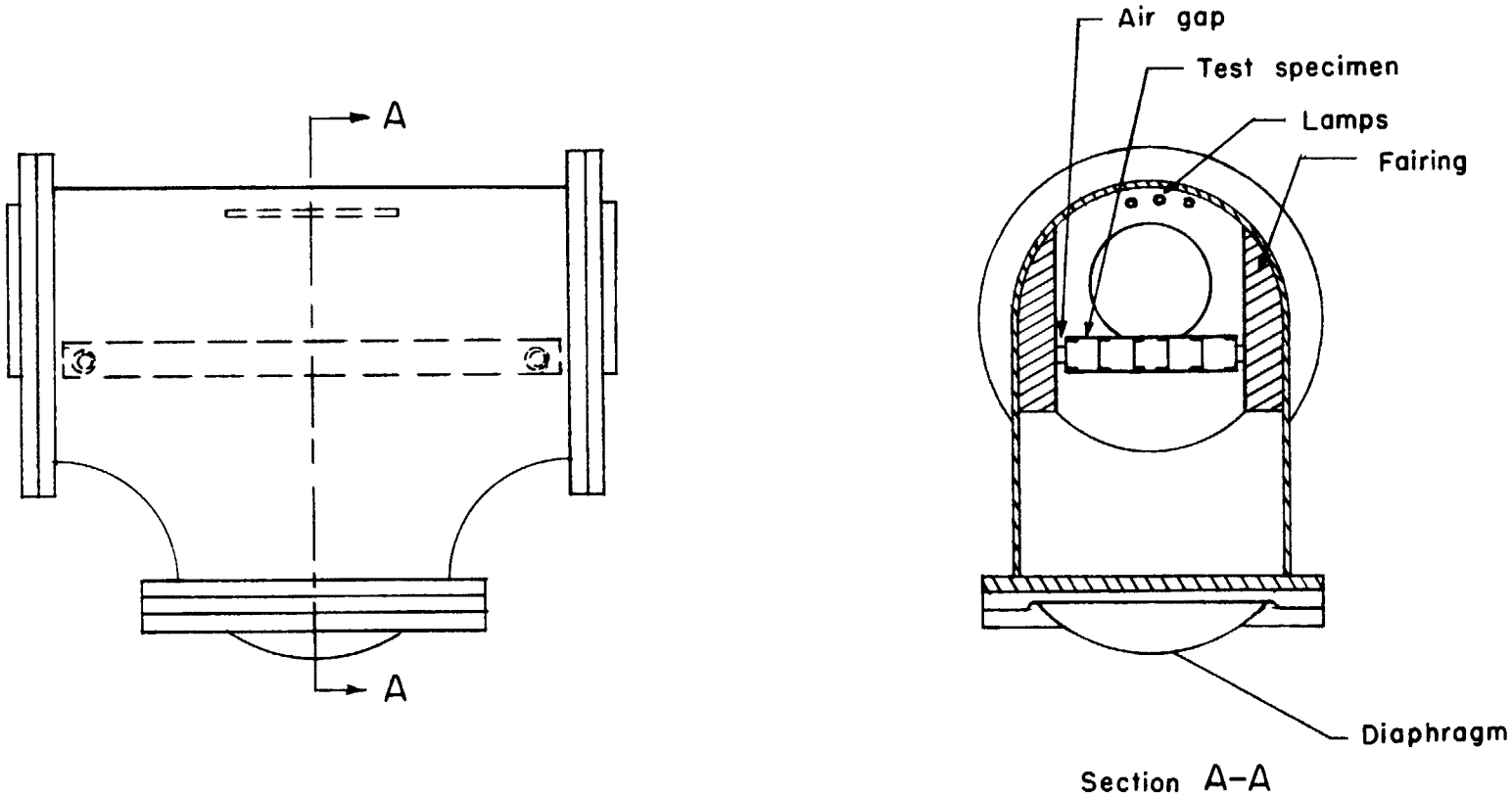

Figure 5.- Sketch of dynamic test chamber.

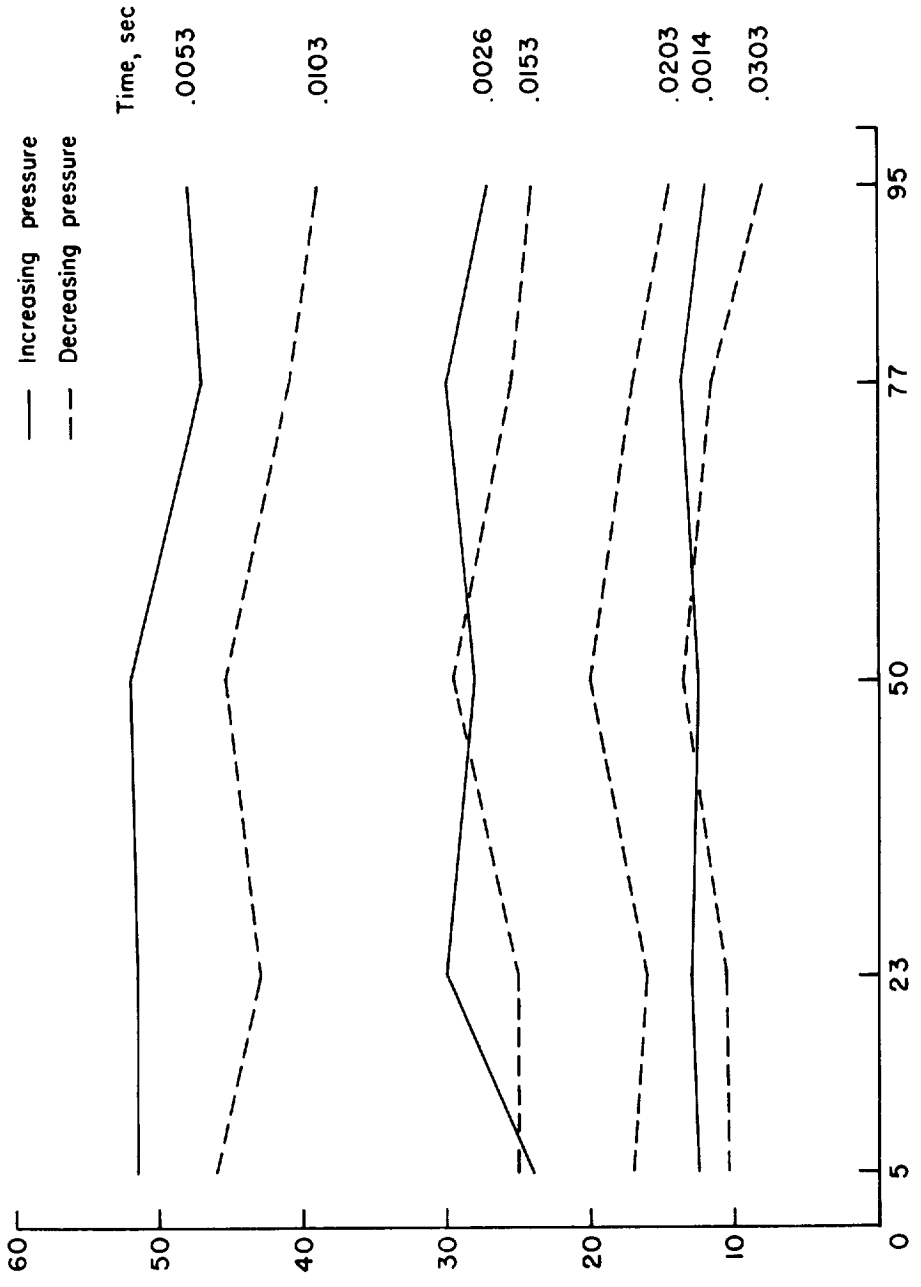

(a) Chordwise variation at midspan.

Figure 6.- Distribution of differential pressure, ΔP, on steel calibration beam. Initial chamber pressure, 74 psi.

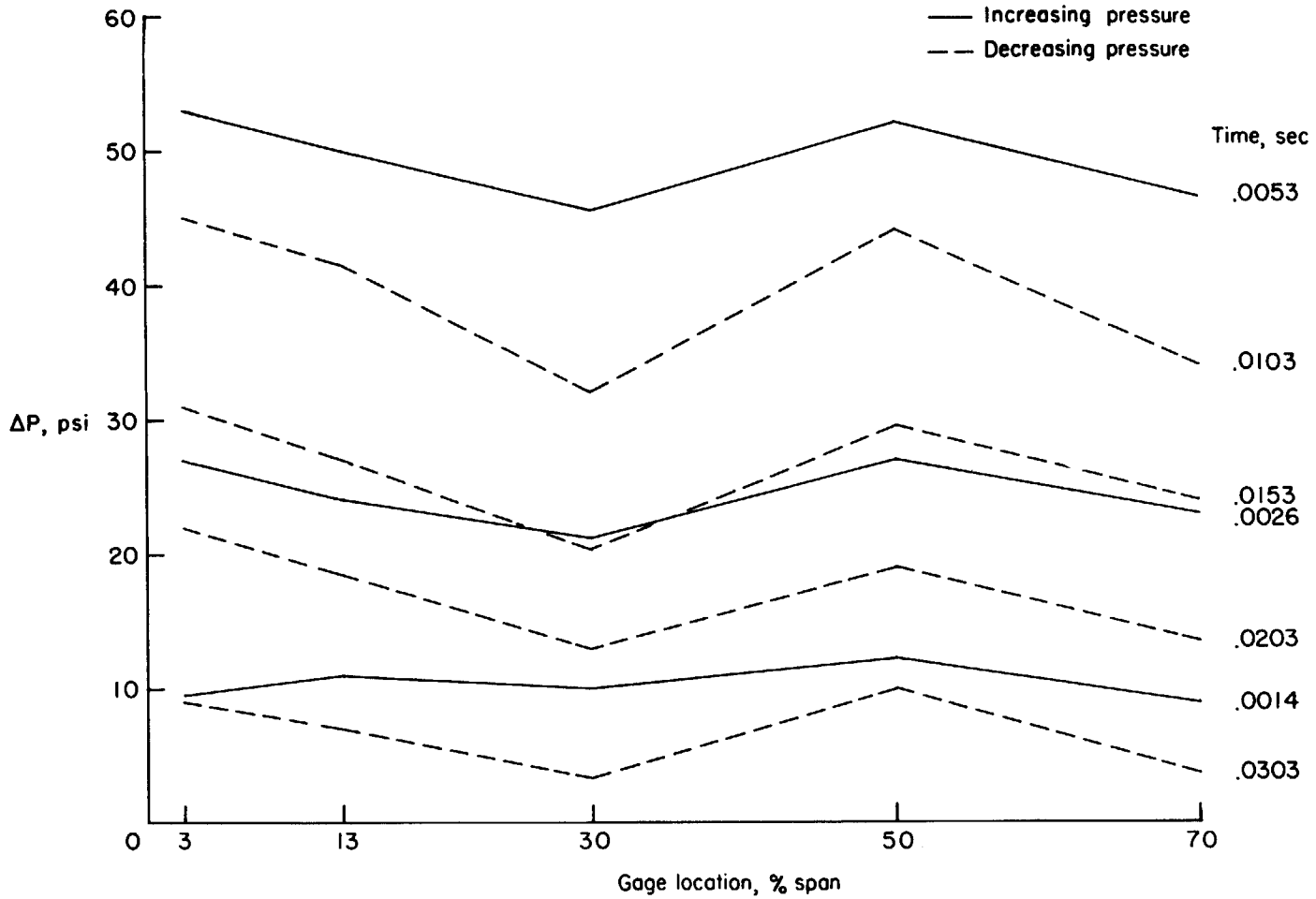

(b) Spanwise variation at midchord.

Figure 6.- Concluded.

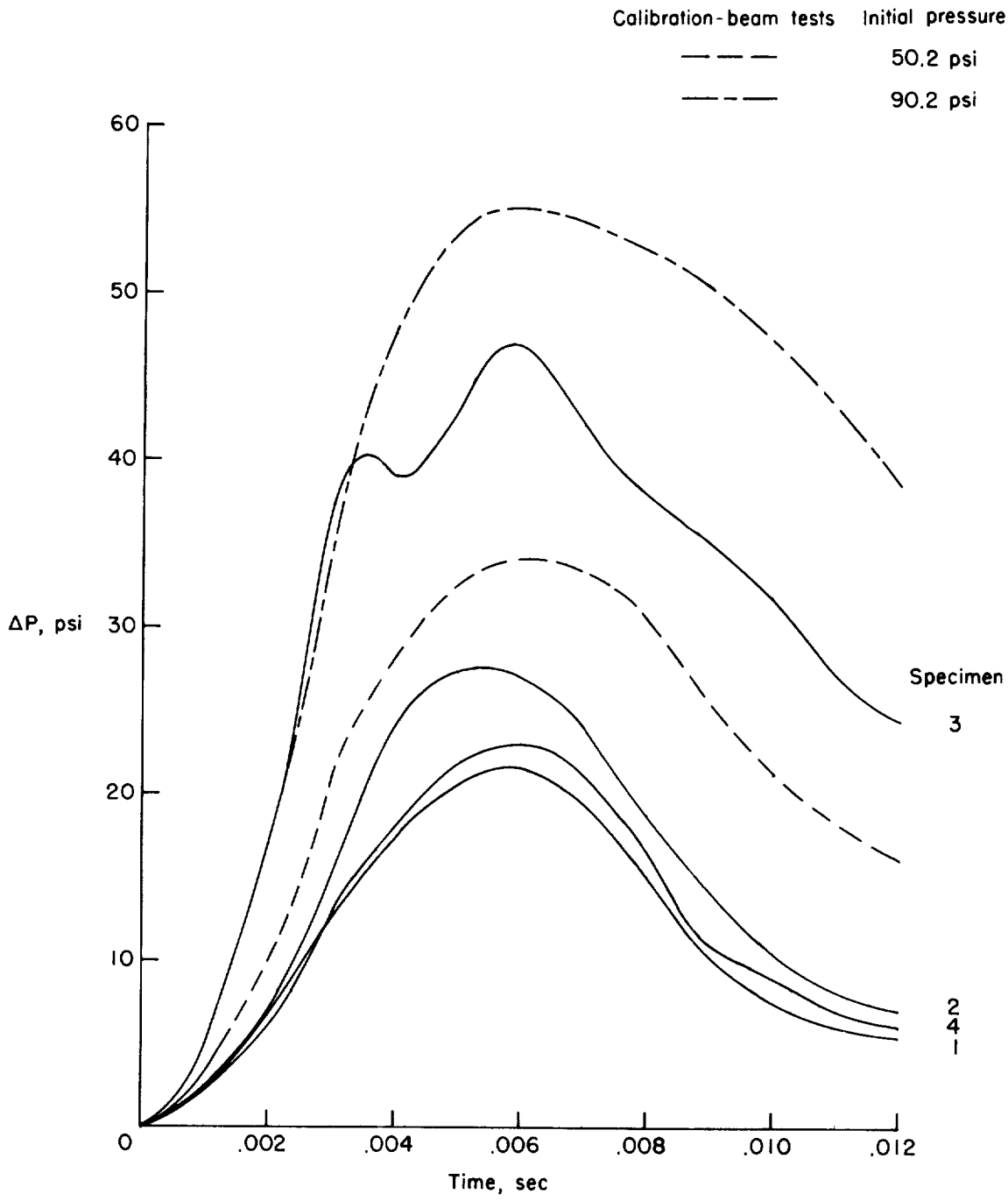

Figure 7.- Histories of differential pressure, ΔP, from tests on steel calibration beam and multiweb beams.

Figure 8.- Test specimen blown from dynamic-test chamber. L-57-983.1

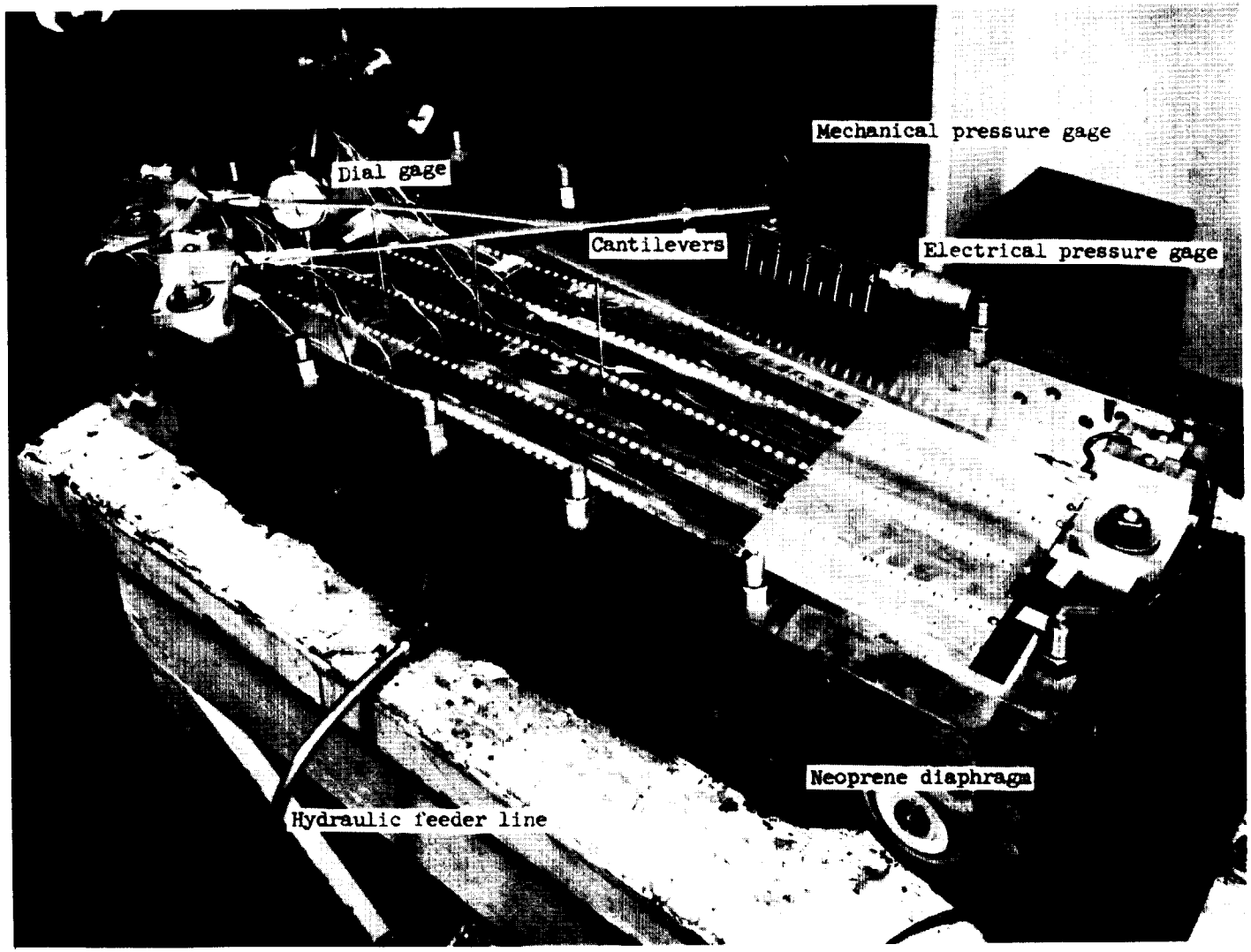

Figure 9.- Static-test fixture containing buckled specimen. L-58-369.1

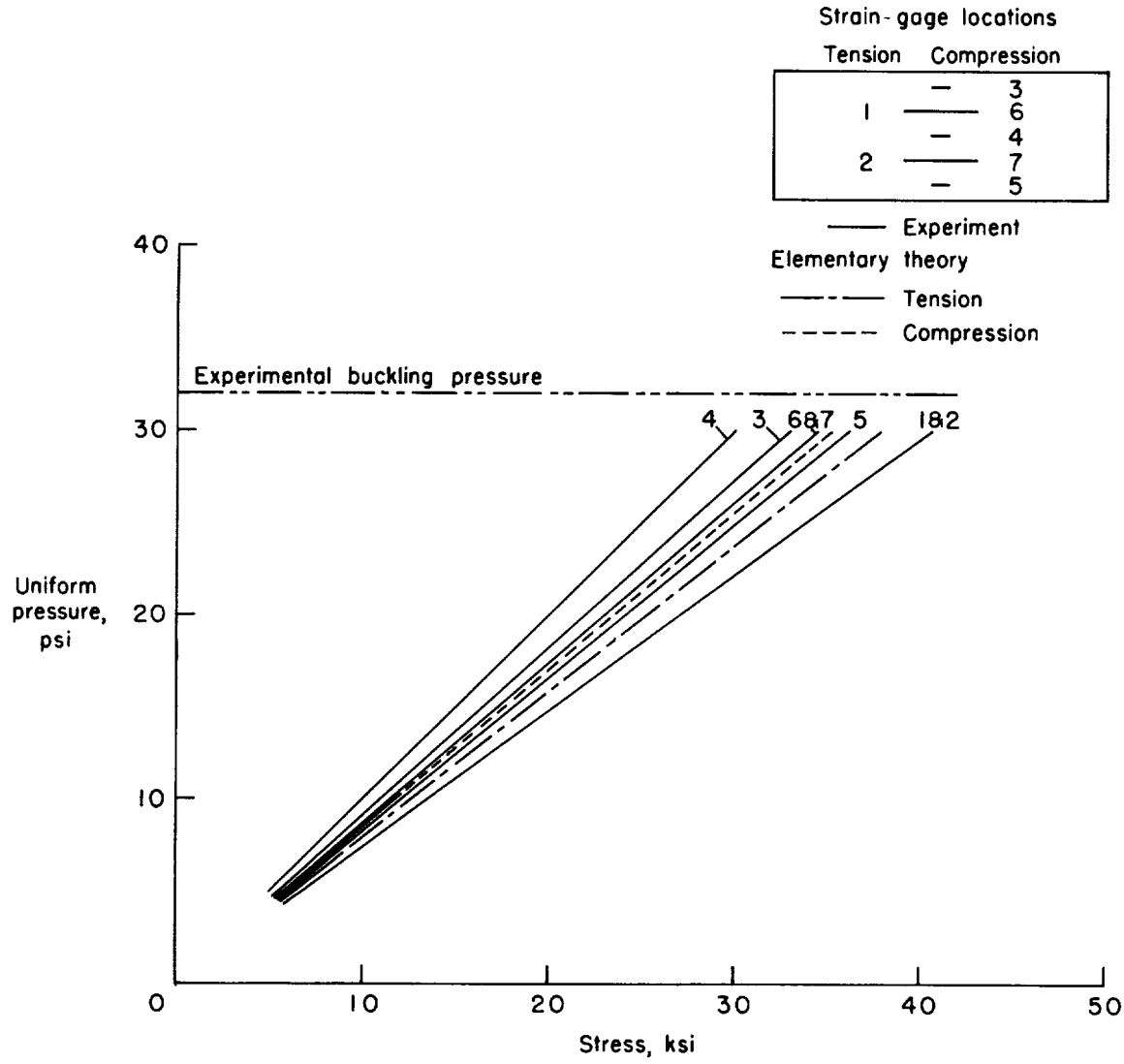

(a) Specimen 1.

Figure 10.- Measured and calculated bending stresses due to static loading in multiweb beams.

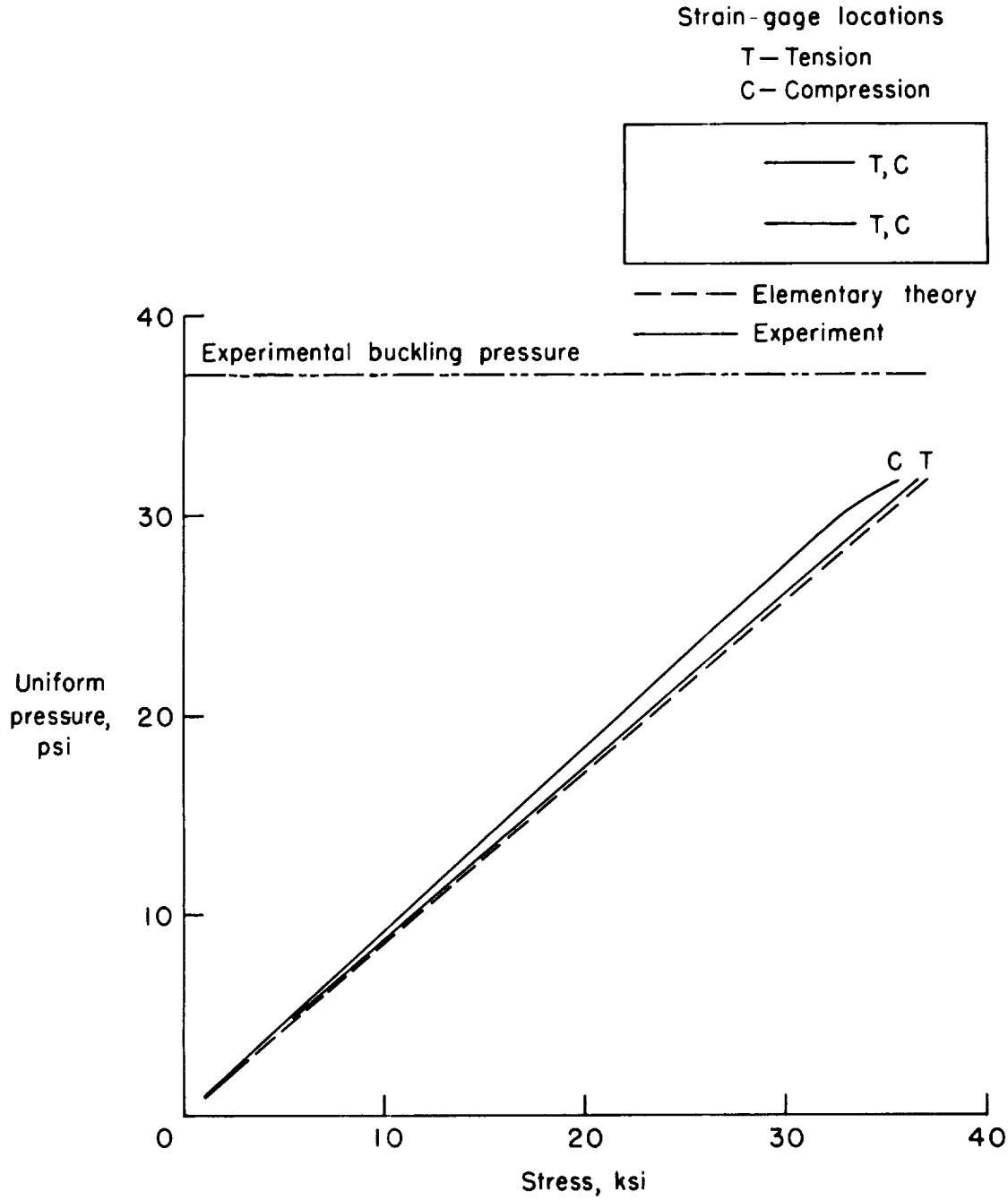

(b) Specimen 2.

Figure 10.- Continued.

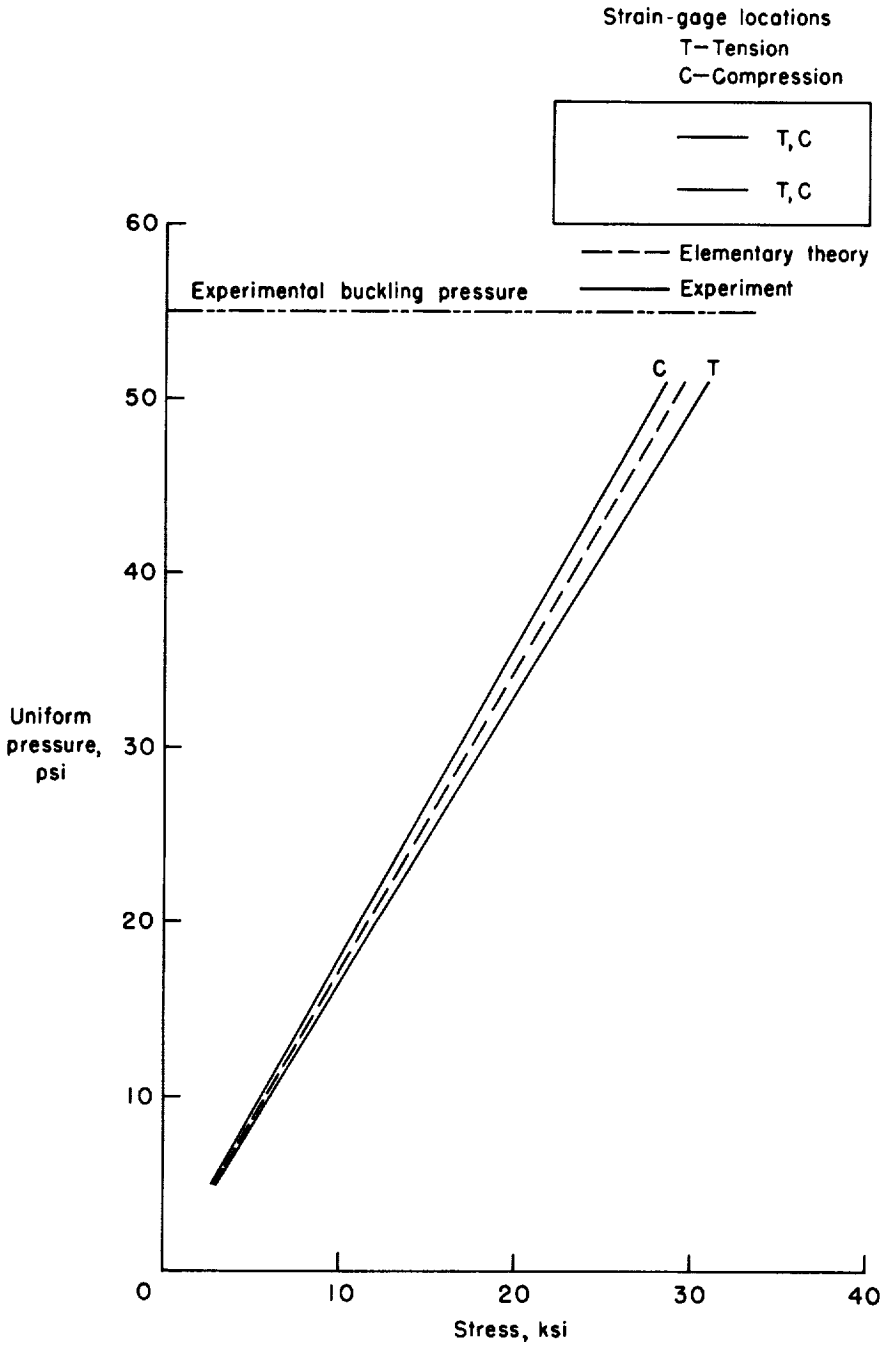

(c) Specimen 3.

Figure 10.- Continued.

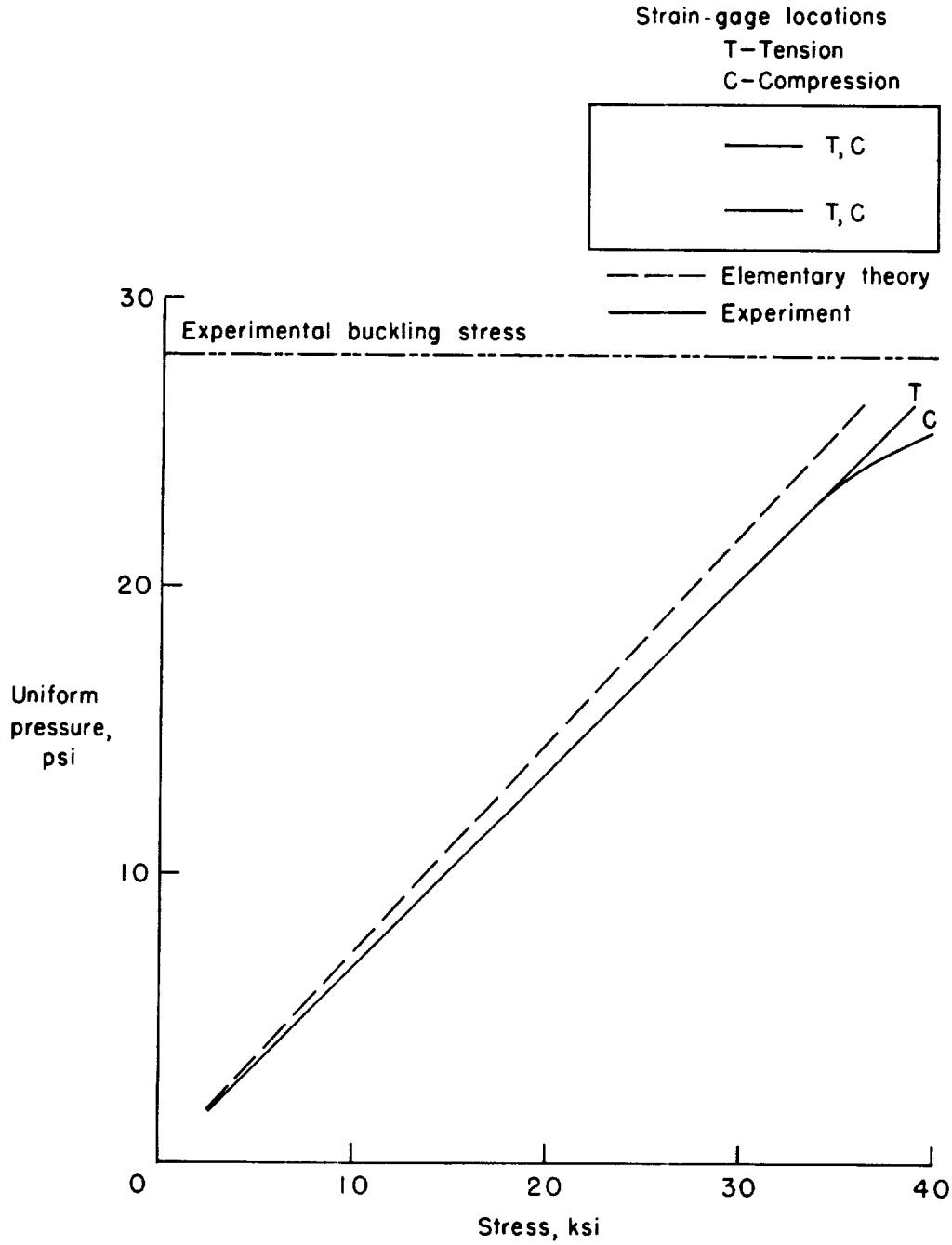

(d) Specimen 4.

Figure 10.- Concluded.

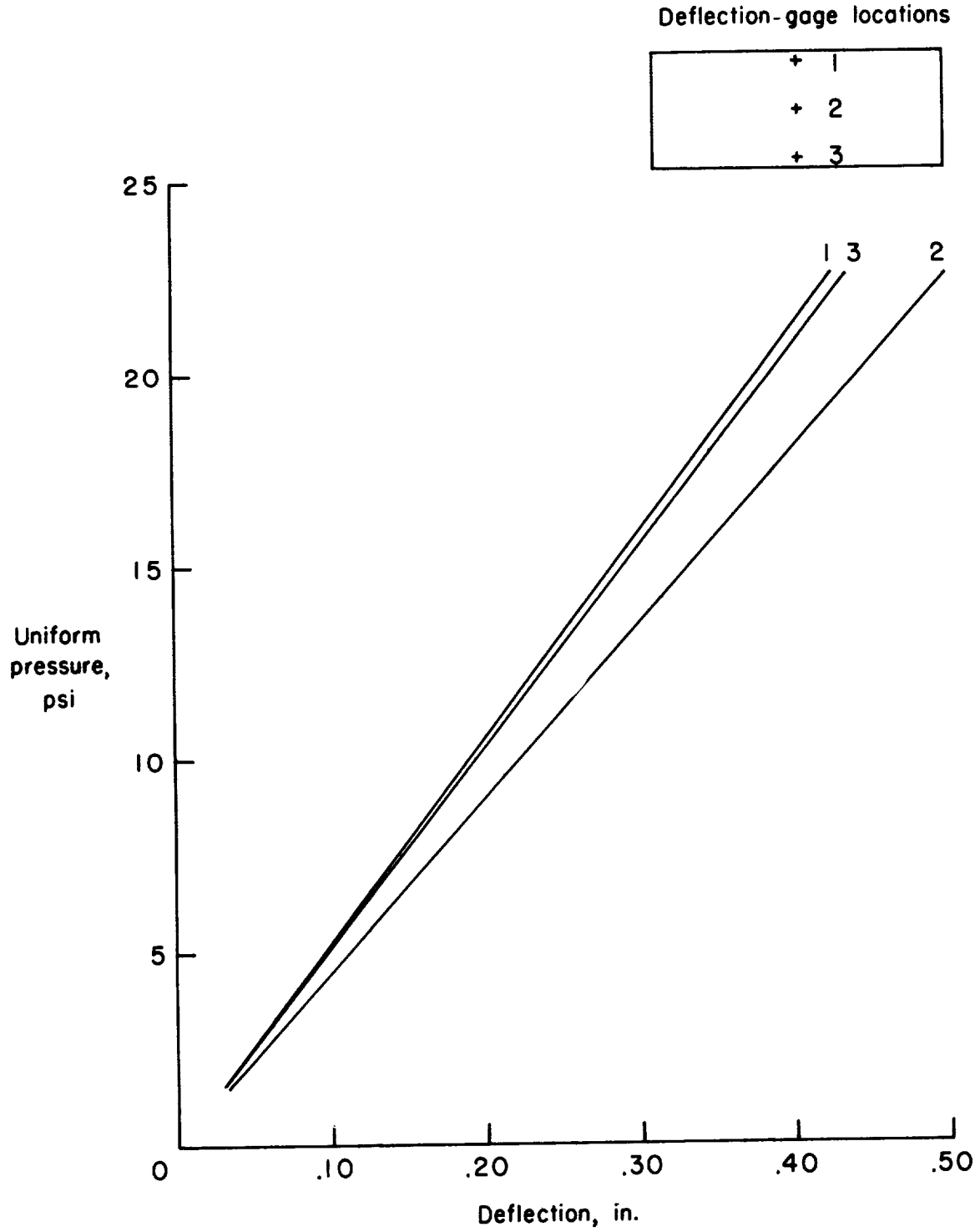

L-1357

Figure 11.- Experimental midspan deflection of specimen 2.

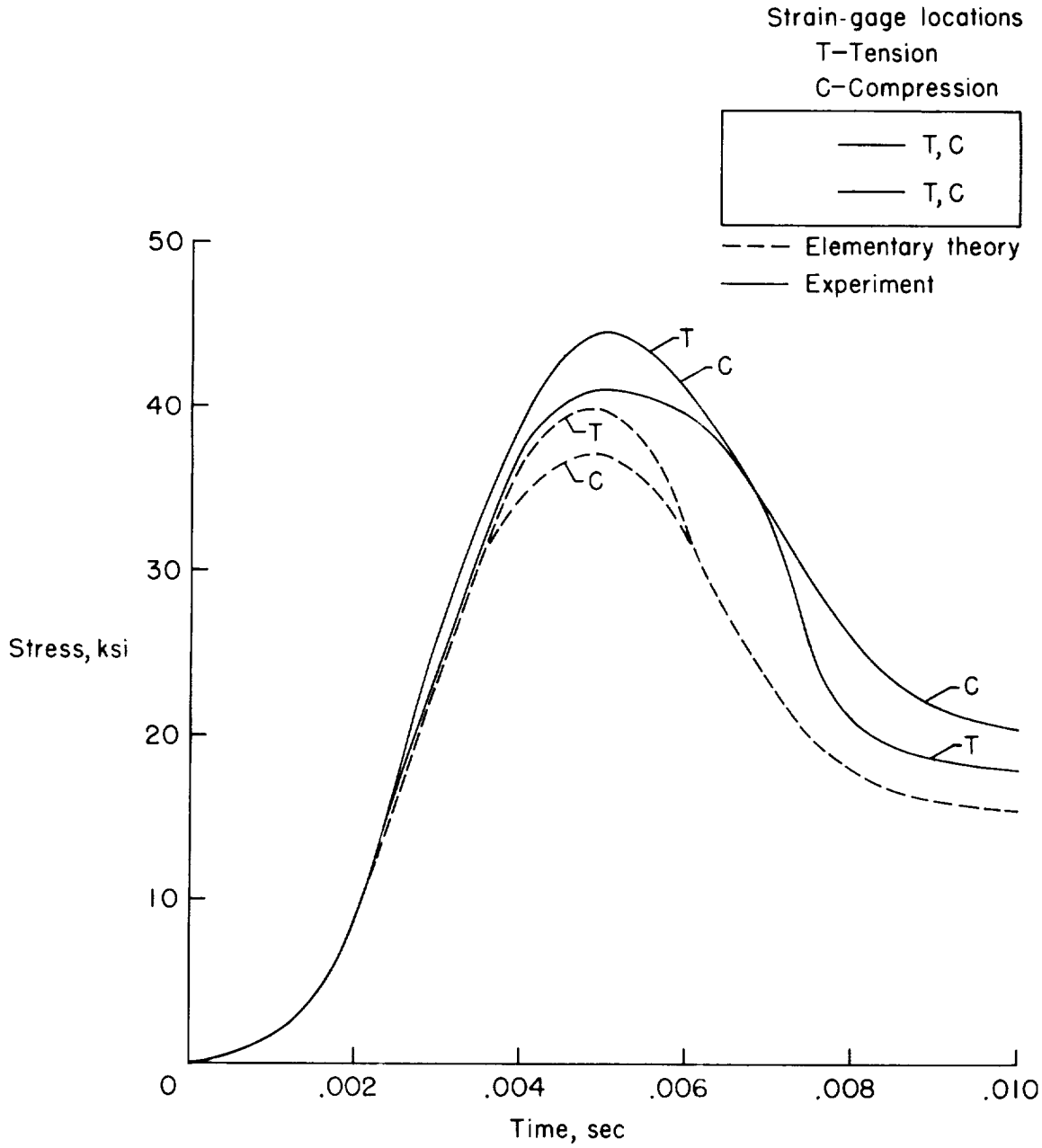

(a) Specimen 1.

Figure 12.- Stress histories from dynamic tests of multiweb beams.

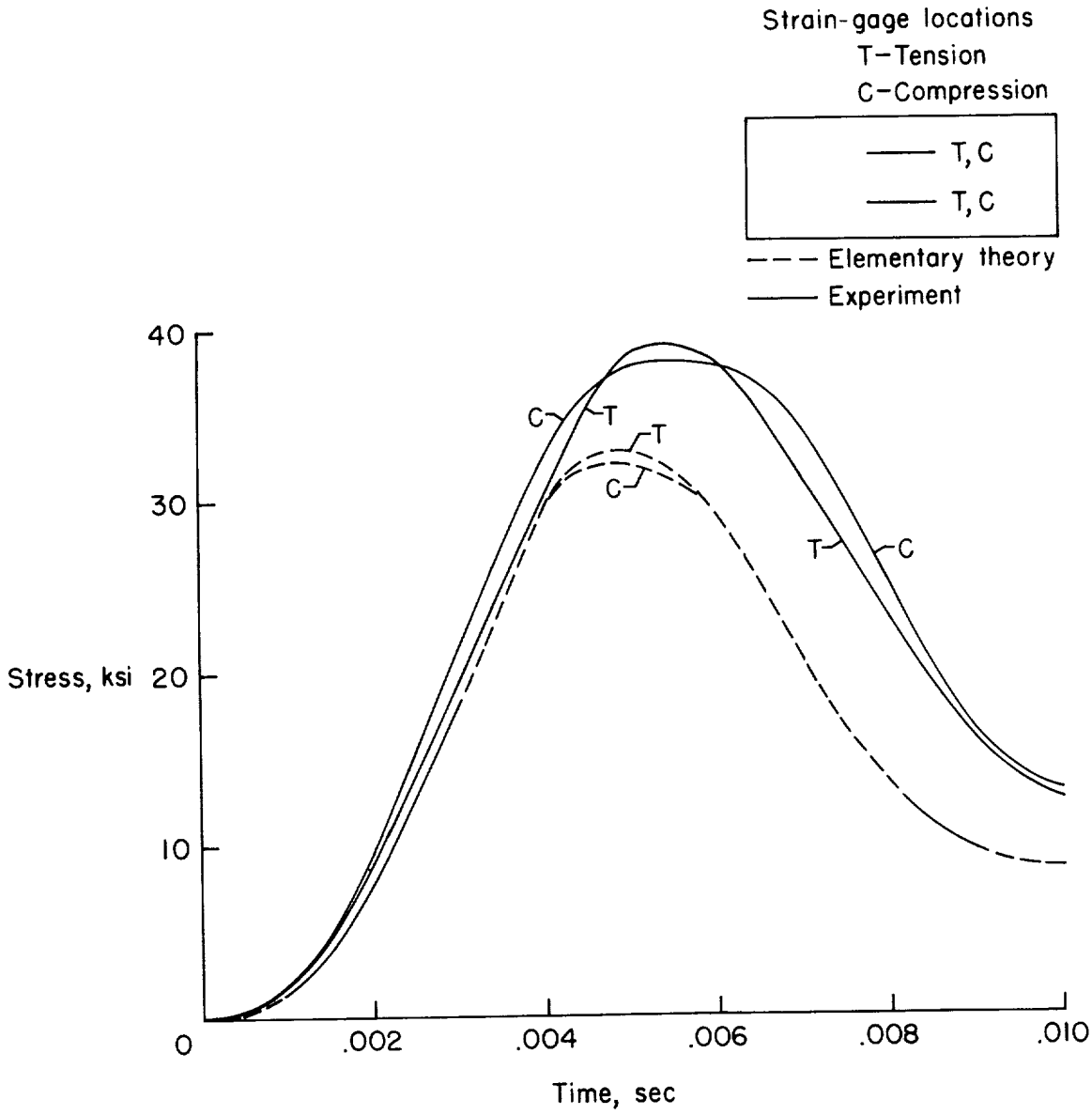

(b) Specimen 2.

Figure 12.- Continued.

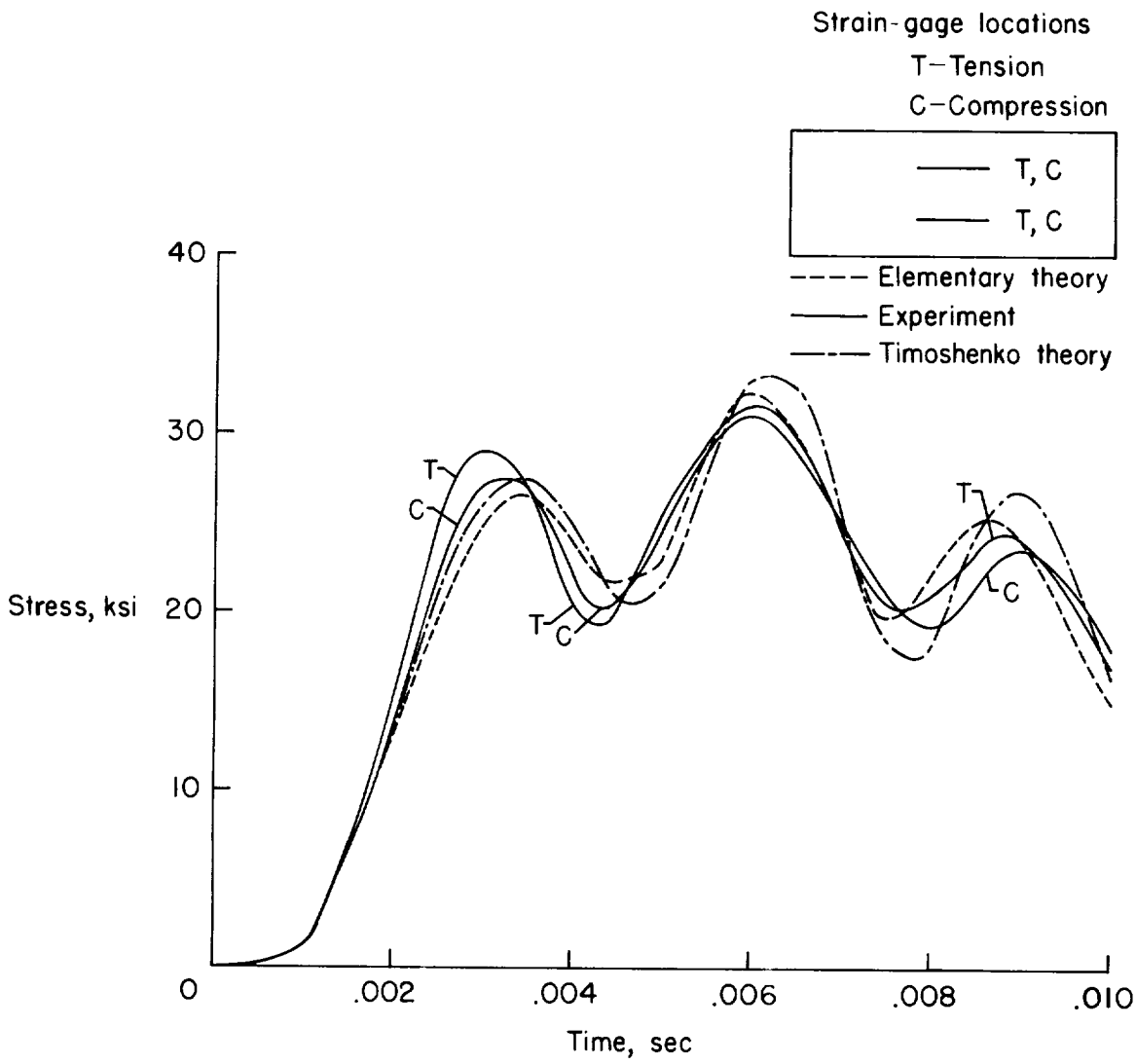

(c) Specimen 3.

Figure 12.- Continued.

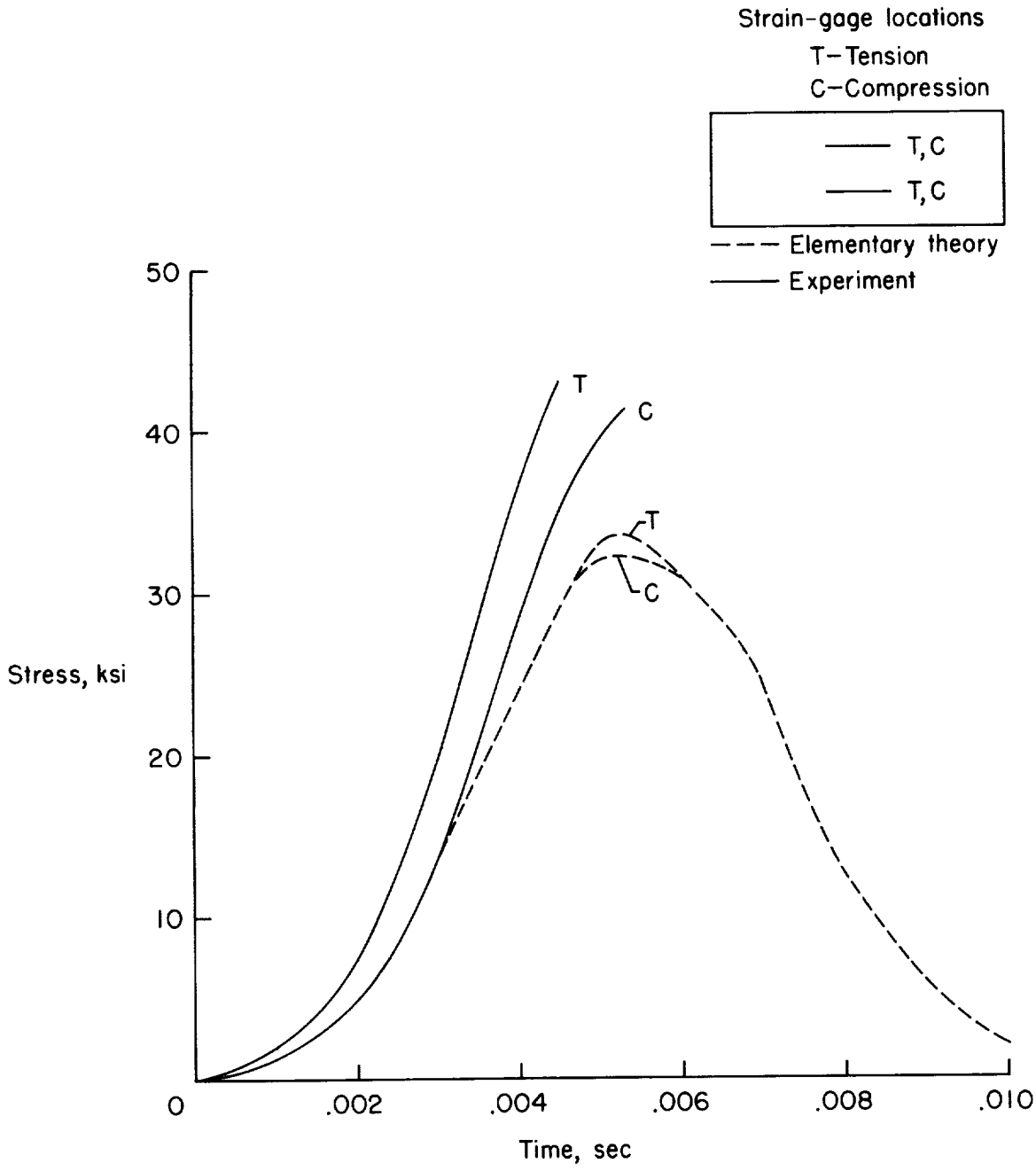

(d) Specimen 4.

Figure 12.- Concluded.

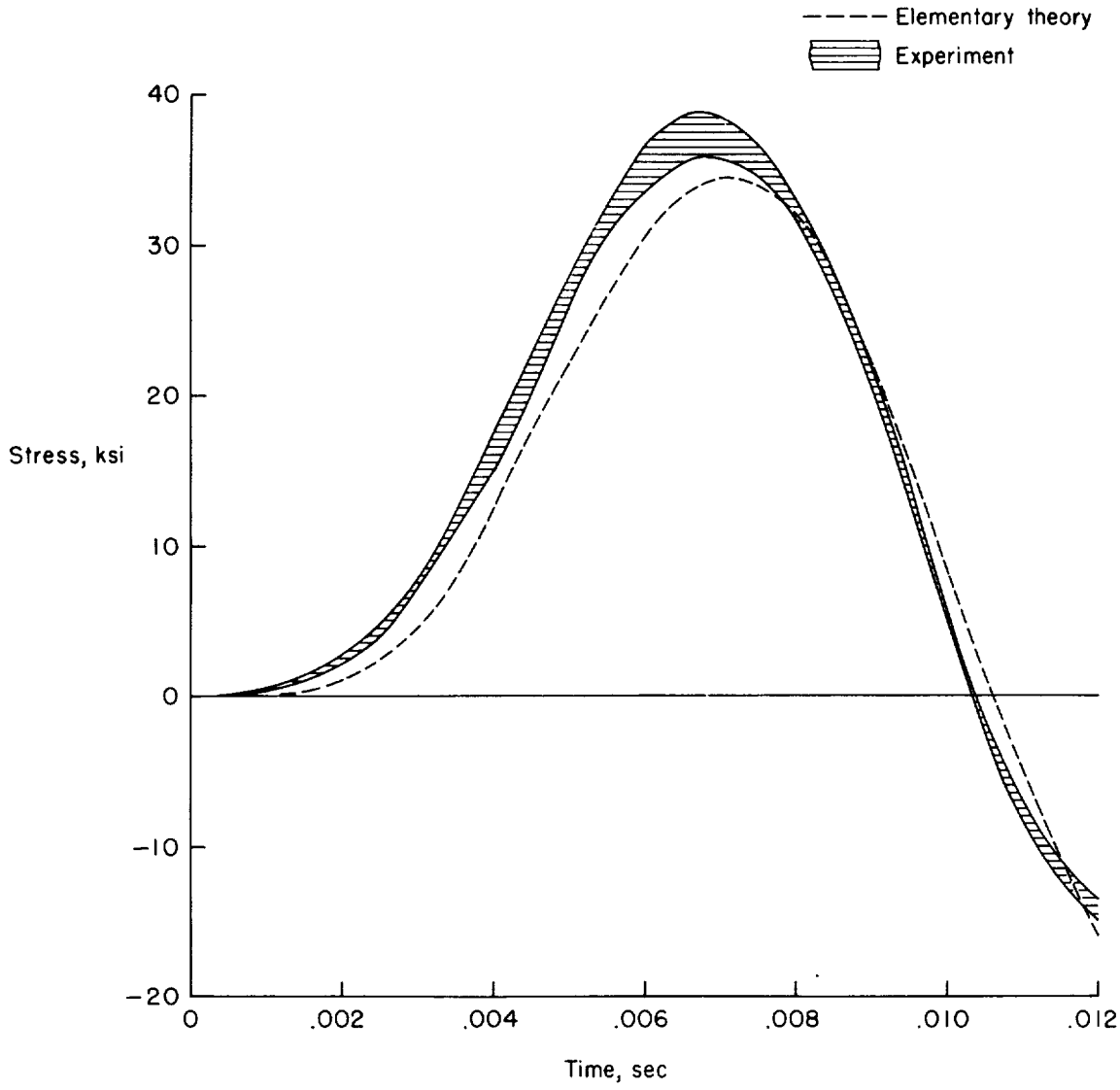

Figure 13.- Stress histories from test on solid aluminum beam. Initial chamber pressure, 33.5 psi; tensile and compressive stresses are plotted in same band.

NASA-Langley, 1962 L-1357